

selection based on feedback processes of genotype replication¹⁹. It is also likely that molecular genotypes and phenotypes may have been the very same molecules²⁰. Our example of a hypercyclic peptide network supports the idea that peptides could play a role in both hypotheses. □

Methods

Self-replication of R₂. All reactions were done in 0.6 ml Eppendorf tubes at 23 °C. A stock solution containing E, N₂ and the internal standard 4-acetamidobenzoic acid (ABA), were seeded with various amounts of R₂. Benzylmercaptan (1 μl) was then added. Reactions were initiated by adding 3-(N-morpholino)propanesulphonic acid (MOPS) buffer (pH = 7.50, 200 mM, 236 μl), giving a total volume of 300 μl and concentrations of [N₂] = 104.5 μM, [E] = 94.2 μM, [R₂] = 0, 4.0, 21.4 or 42.6 μM. [MOPS] = 157 mM, [ABA] = 40.4 μM. Samples (30 μl) were taken at various time points and quenched with 2% trifluoroacetic acid (TFA) in water (70 μl) then stored at -70 °C. Samples were analysed by high pressure liquid chromatography on a Zorbax C8 column using an acetonitrile/water/0.1% TFA gradient while monitoring at 270 nm. The identity of all peptides was determined by mass spectrometry and verified by coinjection with authentic samples. Experiments were done in duplicate.

Determination of hypercyclic organization in the E/N₁/N₂ mixture. Reactions were done as described above except that the stock solution contained, besides E and ABA, both N₁ and N₂, which was subsequently seeded with either R₁, R₂ or water. Reactions were initiated by adding MOPS buffer (pH = 7.50, 200 mM, 236.6 μl), giving a total volume of 300 μl and concentrations of [N₁] = 112.5 μM, [N₂] = 112.7 μM, [E] = 91.1 μM, [MOPS] = 157.7 mM, [ABA] = 97.1 μM, [R₁] = 45.1 μM, [R₂] = 50.4 μM.

Verification of the catalytic components of the hypercycle. Reactions were performed as described above except only one nucleophile was present in the reaction mixture and the reaction was seeded with the replicator that was not produced *in situ*. Initial concentrations are (1) [E] = 88.9 μM, [N₁] = 98.2 μM, [R₂] = 25.2 μM, [ABA] = 50.5 μM; (2) [E] = 80.4 μM, [N₂₁] = 96.9 μM, [R₁] = 35.3 μM, [ABA] = 36.9 μM.

Received 20 June; accepted 20 October 1997.

- Eigen, M. & Schuster, P. The hypercycle. A principle of natural self-organization. Part A: emergence of the hypercycle. *Naturwissenschaften* **64**, 541–565 (1977).
- Eigen, M. & Schuster, P. The hypercycle. A principle of natural self-organization. Part B: the abstract hypercycle. *Naturwissenschaften* **65**, 7–41 (1978).
- Eigen, M. & Schuster, P. The hypercycle. A principle of natural self-organization. Part C: The realistic hypercycle. *Naturwissenschaften* **65**, 341–369 (1978).
- Eigen, M. Self-organization of matter and the evolution of biological macromolecules. *Naturwissenschaften* **58**, 465–523 (1971).
- Müller-Herold, U. What is a hypercycle? *J. Theor. Biol.* **102**, 569–584 (1983).
- Lee, D. H., Severin, K. & Ghadiri, M. R. Autocatalytic networks: the transition from molecular self-replication to molecular ecosystems. *Curr. Opin. Chem. Biol.* (in the press).
- Ricard, J. & Noat, G. Electrostatic effects and the dynamics of enzyme reactions at the surface of plant cells. I. A theory of the ionic control of a complex multi-enzyme system. *Eur. J. Biochem.* **155**, 183–190 (1986).
- Eigen, M., Biebricher, C. K., Gebinoga, M. & Gardiner, W. C. The hypercycle. Coupling of RNA and protein biosynthesis in the infection cycle of an RNA bacteriophage. *Biochemistry* **30**, 11005–11018 (1991).
- Hong, J.-I., Feng, Q., Rotello, V. & Rebek, J. Jr Competition, cooperation and mutation: improving a synthetic replicator by light irradiation. *Science* **255**, 848–850 (1992).
- Achilles, T. & von Kiedrowski, G. A self-replicating system from three starting materials. *Angew. Chem. Int. Edn Engl.* **32**, 1198–1201 (1993).
- Lee, D. H., Granja, J. R., Martinez, J. A., Severin, K. S. & Ghadiri, M. R. A self-replicating peptide. *Nature* **382**, 525–528 (1996).
- Severin, K. S., Lee, D. H., Martinez, J. A. & Ghadiri, M. R. Peptide self-replication via template-directed ligation. *Chem. Eur. J.* **3**, 1017–1024 (1997).
- Harbury, P. B., Zhang, T., Kim, P. S. & Alber, T. A switch between two-, three- and four-stranded coiled coils in GCN4 leucine zipper mutants. *Science* **262**, 1401–1407 (1993).
- Hu, J. C., O'Shea, E. K., Kim, P. S. & Sauer, R. T. Sequence requirements for coiled coils: analysis with λ repressor-GCN4 leucine zipper fusions. *Science* **250**, 1400–1403 (1990).
- Severin, K., Lee, D. H., Martinez, J. A. & Ghadiri, M. R. Dynamic error-correction in an autocatalytic peptide network. *Angew. Chem. Int. Edn Engl.* (in the press).
- von Kiedrowski, G. Minimal replicator theory I: parabolic versus exponential growth. *Bioorg. Chem. Front.* **3**, 113–146 (1993).
- Severin, K., Lee, D. H., Kennan, A. J. & Ghadiri, M. R. A synthetic peptide ligase. *Nature* **389**, 706–709 (1997).
- Kauffman, S. A. *The Origins of Order* (Oxford Univ. Press, New York, 1993).
- Küppers, B.-O. *The Origin of Biological Information* (MIT Press, Cambridge, MA, 1990).
- Joyce, G. F. RNA evolution and the origins of life. *Nature* **338**, 217–224 (1989).

Acknowledgements. We thank K. Kumar for discussions. We also thank the Medical Research Council of Canada for a predoctoral fellowship (D.H.L.), and the Deutsche Forschungsgemeinschaft for a postdoctoral fellowship (K.S.).

Correspondence and requests for materials should be addressed to M.R.G. (e-mail: ghadiri@scripps.edu).

Kinetic limitations on droplet formation in clouds

P. Y. Chuang*, R. J. Charlson† & J. H. Seinfeld‡

* Department of Environmental Engineering Science, MC 138-78, California Institute of Technology, Pasadena, California 91125, USA

† Departments of Atmospheric Sciences and Chemistry, University of Washington, Seattle, Washington 98195, USA

‡ Division of Engineering and Applied Science and Department of Chemical Engineering, MC 210-41, California Institute of Technology, Pasadena, California 91125, USA

The 'indirect' radiative cooling of climate due to the role of anthropogenic aerosols in cloud droplet formation processes (which affect cloud albedo) is potentially large, up to -1.5 W m^{-2} (ref. 1). It is important to be able to determine the number concentration of cloud droplets to within a few per cent, as radiative forcing as a result of clouds is very sensitive to changes in this quantity², but empirical approaches are problematic^{3–5}. The initial growth of a subset of particles known as cloud condensation nuclei and their subsequent 'activation' to form droplets are generally calculated with the assumption that cloud droplet activation occurs as an equilibrium process described by classical Köhler theory^{6,7}. Here we show that this assumption can be invalid under certain realistic conditions. We conclude that the poor empirical correlation between cloud droplet and cloud condensation nuclei concentrations is partly a result of kinetically limited growth before droplet activation occurs. Ignoring these considerations in calculations of total cloud radiative forcing based on cloud condensation nuclei concentrations could lead to errors that are of the same order of magnitude as the total anthropogenic greenhouse-gas radiative forcing¹.

Cloud droplet activation and subsequent treatments of cloud droplet growth in atmospheric models generally rely on the assumption that pre-activation growth is accurately described by an equilibrium model in which the particle diameter is always at equilibrium with the local supersaturation^{6,7}. The equilibrium relationship between supersaturation and particle size for a particle composed of highly soluble inorganic species can be described by the well-known Köhler equation (curve A, Fig. 1)⁸. Cloud droplet nuclei (CDN) activate when they grow larger than their critical diameter, D_{pc} , after which they can grow spontaneously, limited only by growth kinetics. The concept of CDN is distinct from that of CCN in that, whereas CCN are defined as those particles that activate to become cloud droplets within a cloud chamber of fixed or prescribed supersaturation, CDN are those particles that actually activate in the atmosphere under conditions of time-varying supersaturation.

To evaluate the conditions under which the equilibrium activation model is valid, two timescales will be defined. One is the timescale for particle growth that would be required for that particle to remain at equilibrium as the ambient supersaturation ratio increases in a rising air parcel, τ_e . The other is the timescale for actual change in the droplet size resulting from condensational growth, τ_g . Hence, if $\tau_e \gg \tau_g$ then the equilibrium model is reasonable; otherwise, CDN activation, and hence the cloud droplet size distribution, can be accurately predicted only if the kinetics of droplet growth are considered. To calculate τ_e , the rate of change of the droplet diameter that would be required for that droplet to remain at its equilibrium size, dD_{pe}/dt , is determined from the combination of two effects. First, the time rate of change of supersaturation, dS/dt , can be determined using a simple one-dimensional adiabatic parcel model⁹. Next, the rate of change of D_{pe} with respect to supersaturation, dD_{pe}/dS , is determined by differentiating

the Köhler relationship. Combining these two expressions yields $dD_{pe}/dt = (dD_{pe}/dS)(dS/dt)$, after which τ_e can be determined from $\tau_e = D_{pe}/(dD_{pe}/dt)$. Similarly, the time rate of change of the particle diameter resulting from condensational growth, dD_{pg}/dt , can be computed using established expressions^{10,11}, after which τ_g can be determined from $\tau_g = D_{pg}/(dD_{pg}/dt)$.

Figure 2 shows the two timescales as a function of particle critical supersaturation S_c . The base-case parameters given in the figure were estimated for typical marine stratiform clouds⁹, which are climatically the most important cloud type². The most notable feature of Fig. 2 is that for $S_c < 0.042\%$, $\tau_g \gg \tau_e$; that is, these pre-activated droplets do not grow sufficiently quickly to follow the changes in the equilibrium diameter, implying that for particles with $S_c < 0.042\%$ (for example, pure NH_4HSO_4 particles of size $>0.23 \mu\text{m}$ dry diameter), condensational growth kinetics are important. The fraction of CCN in this regime can be estimated using the common empirical parameterization of the cumulative CCN spectrum, $N = CS^k$, where N is the CCN number concentration, S is the supersaturation, and C and k are empirically determined parameters¹². If the peak supersaturation achieved in an air parcel is S_{max} , the fraction of CCN for which growth kinetics are important is $(S_c^*/S_{\text{max}})^k$, where S_c^* is the value of S_c at which $\tau_g = \tau_e$. When this fraction is significant, accurately predicting cloud droplet size distributions requires a kinetic description of CDN pre-activation growth. Assuming a value of S_{max} of 0.1%, this fraction is 0.76, 0.63 and 0.53 for k values of 0.3, 0.5, and 0.7, respectively, for the base case of Fig. 2. These exponents are representative of data from observations of marine stratiform clouds¹².

The sensitivity of S_c^* to temperature, pressure, droplet diameter, updraft velocity, and thermal and mass accommodation coefficients (these coefficients represent the fractions of gas-particle collisions that result in actual transfer) is presented in Fig. 3. The base case is seen actually to be a conservative estimate of S_c^* , as almost all the values in Fig. 3 lie above $S_c^* = 0.042\%$. Changes in pressure and temperature do not greatly affect S_c^* . Changes in the updraft velocity are more significant, as dS/dt is directly proportional to this quantity. S_c^* is sensitive to changes in the accommodation coefficients only if α_c or α_t is less than 0.1. Values for α_c in the range of 0.03 to 1.0 have been reported¹³. S_c^* is most sensitive to the particle diameter (increasing by more than a factor of 2 for a 50% change in diameter)

primarily because τ_g is directly proportional to D_p^2 . This implies that a particle that began in the equilibrium regime may, through condensational growth, cross over into the kinetic regime while it is still unactivated, indicating that the fraction of particles for which growth kinetics is important is even higher than estimated in the base case.

There is initial evidence that organic compounds make up a significant fraction of CCN mass^{14,15} and can alter a particle's Köhler curve¹⁶. The effect of organics on τ_e and τ_g can be divided into three distinct factors: (1) changes in the droplet surface tension; (2) gradual dissolution of solute due to limited solubility; and (3) changes in the mass accommodation coefficient.

The presence of water-soluble organics decreases in varying amounts the surface tension of these solutions¹⁶. In the absence of any other perturbations, a decrease in the droplet surface tension σ by $\Delta\sigma$ can be shown to decrease the critical diameter by a factor of $\Delta\sigma/\sigma$, as illustrated by curves A and B in Fig. 1. One consequence of this decrease is to increase τ_e because at a given value of S , curve B is shifted to smaller sizes relative to curve A, which causes a decrease in dD_{pe}/dS . Another consequence is that τ_g decreases by roughly $2\Delta\sigma/\sigma$ because τ_g is directly proportional to D_p^2 . The combination of these effects shifts S_c^* to smaller values. Using the base-case parameters, for $\Delta\sigma/\sigma = 15\%$, τ_e increases by about 15%, τ_g decreases by 28%, and S_c^* decreases by 11%. As a result, the fraction of particles in the kinetic regime decreases by 6%.

If the solubility limit of the organic fraction in a droplet is reached, then the amount of solute within that droplet increases as the droplet grows in order to maintain saturated conditions. Qualitatively, the gradual dissolution of organics broadens the Köhler curve as illustrated in curve C, Fig. 1. In some cases, local maxima and minima can arise in the Köhler curve when organic components fully dissolve¹⁶. The overall effect of gradual dissolution on both time constants seems to be small compared with surface tension effects for realistic conditions. We do not consider here a possibly related influence, the kinetics of dissolution.

It has already been shown that S_c^* changes rapidly with changes in the condensation coefficient α_c for $\alpha_c \leq 0.1$ as a result of changes in τ_g . Many organic compounds can be present at the solution/air interface in quantities in excess of the bulk average as a result of their partially hydrophobic nature¹⁷. Organics can change the evaporative

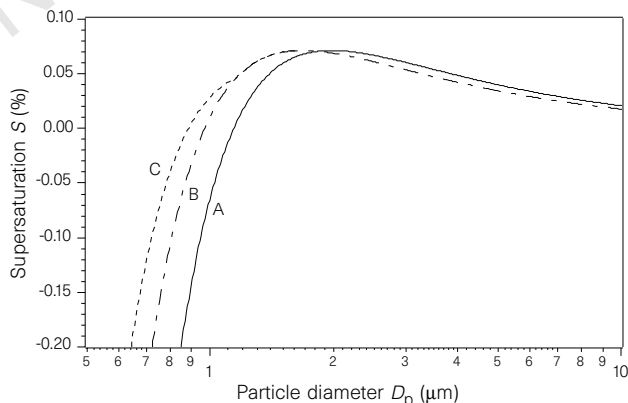


Figure 1 Köhler curves for three different particles. All curves are for $S_c = 0.071\%$. For curve A, $\sigma = \sigma_{\text{water}}$, and the solute is infinitely soluble. For curve B, σ is lower because of the presence of an organic species, so $\sigma = 0.85 \sigma_{\text{water}}$, but the solute is still infinitely soluble. Curve C is as curve B, except the organic solubility is assumed to be 0.02M. D_{pc} shifts from 1.97 μm in curve A to 1.67 μm in curves B and C because of the surface tension decrease. Curves B and C join together when the organic fraction of curve C fully dissolves.

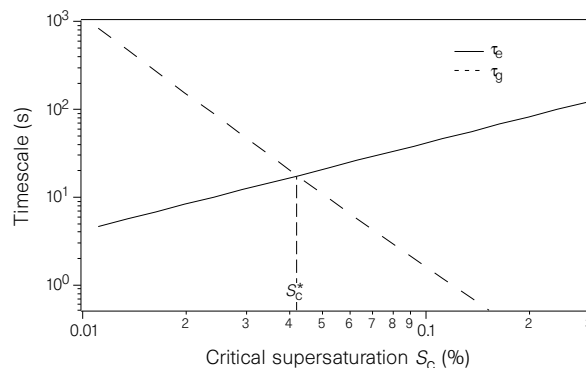


Figure 2 Base-case comparison of the equilibrium (τ_e) and droplet growth (τ_g) timescales as a function of critical supersaturation. Base-case parameters are temperature $T = 280 \text{ K}$, pressure $p = 900 \text{ mbar}$, updraft velocity $u = 20 \text{ cm s}^{-1}$, and mass (α_c) and thermal (α_t) accommodation coefficients equal to unity. To calculate the timescales, a diameter must be specified; the equilibrium diameter at 100% relative humidity was chosen for the base case. It can be seen that S_c^* is a good indicator of the transition from kinetic to equilibrium regimes because the ratio τ_e/τ_g is a strong function of critical supersaturation. Note that there is an inverse relationship between S_c and particle diameter. For example, an ammonium bisulphate particle with $S_c = 0.01\%$ has a dry diameter of 0.6 μm , and for $S_c = 0.2\%$, dry particle diameter is 0.09 μm .

properties of bulk water even in minute quantities¹⁸. Therefore, it seems plausible at least that organics could cause substantial changes in α_c , and therefore S_c^* , although no attempt at quantifying such an effect will be made here.

There do not seem to be any observations of CDN and cloud droplets where the full set of possible controlling variables has been measured. It may not in fact be possible at present to make the necessary measurements *in situ* that could support or negate the above model calculations. However, there is evidence that cloud droplet growth can be delayed in cloud chambers¹⁹. The effect has been attributed to the presence of an organic coating¹⁹, but kinetic variations of activation could also explain these observations.

Neglecting kinetic limitations on pre-activation droplet growth has direct consequences for models of cloud droplet populations, and therefore cloud radiative climate forcing. First, models that use an equilibrium assumption such as $N = CS^k$ must overestimate the droplet number concentration that actually would form, because kinetically limited growth means that some of those droplets fail to activate. To estimate the error in cloud droplet concentration and hence the magnitude by which the equilibrium activation model overestimates cloud radiative forcing, we compare results from the approximation $N = CS^k$ with those from a one-dimensional adiabatic cloud model that includes explicit pre-activation growth kinetics⁹. Using the above base case, and for $k = 0.3, 0.5$ and 0.7 , the equilibrium model estimates CDN concentrations ([CDN]) to be 69%, 29% and 14%, higher respectively, than the cloud model. These differences in [CDN] can be translated into estimates of the overprediction of globally averaged cloud forcing using a previously published relationship between global-mean cloud radiative forcing and [CDN] changes². On the basis of this calculation, the equilibrium activation model overestimates the magnitude of the total (natural plus anthropogenic) cloud radiative forcing by 3.6, 1.8 and 0.9 W m^{-2} , respectively, which are significant compared with the total estimated greenhouse forcing¹ of 2.4 W m^{-2} . Although these numbers are approximate, it is clear from their magnitude that climate models must consider activation kinetics in order to accurately predict the radiative climate forcing by clouds.

Another consequence of kinetically limited activation is that CCN chambers that have residence times that differ from typical growth times found in real clouds will incorrectly measure the CDN concentration. Figure 2 shows typical activation timescales between a fraction of a second and hundreds of seconds, whereas cloud chambers tend to have residence times of a few seconds to a few tens

of seconds. The measured CCN concentration will be either too small or too large, depending on whether the CCN instrument had a growth time that was shorter or longer than that in the actual cloud. In either case, the data will not be appropriate for use with climate models unless the discrepancy is considered. CCN measurements under conditions that mimic cloud conditions would yield data more useful for calculations of cloud radiative forcing. □

Received 20 January; accepted 13 October 1997.

- Intergovernmental Panel on Climate Change *Climate Change 1995: The Science of Climate Change* (eds Houghton, J. T. et al.) 3–7 (Cambridge Univ. Press, Cambridge, 1996).
- Charlson, R. J. et al. Climate forcing by anthropogenic aerosols. *Science* **255**, 423–430 (1992).
- Twomey, S. & Warner, J. Comparison of measurements of cloud droplets and cloud nuclei. *J. Atmos. Sci.* **24**, 702–703 (1967).
- Hegg, D. A., Ferek, R. J. & Hobbs, P. V. Light-scattering and cloud condensation nucleus activity of sulfate aerosol measured over the Northeast Atlantic Ocean. *J. Geophys. Res.* **98**, 14887–14894 (1993).
- Pueschel, R. F. et al. Aerosols in polluted versus nonpolluted air masses—long-range transport and effects on clouds. *J. Clim. Appl. Meteorol.* **25**, 1908–1917 (1986).
- Schwartz, S. E. et al. in *Aerosol Forcing of Climate* (eds Charlson, R. J. & Heintzenberg, J.) 251–280 (Wiley, Chichester, 1995).
- Ghan, S. J. et al. A parameterization of cloud droplet nucleation part I: single aerosol type. *Atmos. Res.* **30**, 197–221 (1993).
- Seinfeld, J. H. *Atmospheric Chemistry and Physics of Air Pollution* (Wiley, New York, 1986).
- Jensen, J. B. & Charlson, R. J. On the efficiency of nucleation scavenging. *Tellus B* **36**, 367–375 (1984).
- Pruppacher, H. R. & Klett, J. D. *Microphysics of Clouds and Precipitation* (Reidel, Dordrecht, 1978).
- Fukuta, N. & Walter, A. Kinetics of hydrometeor growth from a vapor-spherical model. *J. Atmos. Sci.* **27**, 1160–1172 (1970).
- Hobbs, P. V. in *Aerosol-Cloud-Climate Interactions* (ed. Hobbs, P. V.) 33–37 (Academic, San Diego, 1993).
- Mozurkewich, M. Aerosol growth and the condensation coefficient for water: a review. *Aerosol Sci. Technol.* **5**, 223–236 (1986).
- Novakov, T. & Penner, J. E. Large contribution of organic aerosols to cloud-condensation-nuclei concentrations. *Nature* **365**, 823–826 (1993).
- Rivera-Carpio, C. A. et al. Derivation of contributions of sulfate and carbonaceous aerosols to cloud condensation nuclei from mass size distributions. *J. Geophys. Res.* **101**, 19483–19493 (1996).
- Shulman, M. L. et al. Dissolution behavior and surface tension effects of organic compounds in nucleating cloud droplets. *Geophys. Res. Lett.* **23**, 227–280 (1996).
- Stumm, W. & Morgan, J. J. *Aquatic Chemistry* (Wiley, New York, 1981).
- Barnes, G. T. & La Mer, V. K. in *Retardation of Evaporation by Monolayers: Transport Processes* (ed. La Mer, V. K.) 9–33 (Academic, New York, 1962).
- Bigg, E. K. Discrepancy between observation and prediction of concentrations of cloud condensation nuclei. *Atmos. Res.* **20**, 82–86 (1986).

Acknowledgements. This work was supported by the Office of Naval Research and the National Science Foundation.

Correspondence should be addressed to J.H.S. (e-mail: seinfeld@cco.caltech.edu).

Vanishing atomic migration barrier in SiO₂

Michael J. Aziz*, Susan Circone† & Carl B. Agee†

* Division of Engineering and Applied Sciences, † Department of Earth and Planetary Sciences, Harvard University, Cambridge, Massachusetts 02138, USA

Understanding the high-pressure behaviour of SiO₂, a prototypical network-forming material, is important for resolving many problems in the Earth sciences. For pressures of 1–3 GPa (~1–3 × 10⁴ atm), it has been shown that increases in pressure result in higher rate constants for atomic transport processes such as diffusion, viscous flow and crystal growth in SiO₂ as well as in some silicate melts^{1–5}. Structural transitions and coordination changes observed beyond 10 GPa (refs 5–9) may also be related to this pressure-induced increase in atomic mobility. There must be limits, however, on the extent to which pressure can enhance mobility, as a migration barrier decreasing linearly with pressure should vanish at a critical pressure, beyond which a sudden change in behaviour should be observed^{10,11}. Here we report measurements of the pressure dependence of the growth rate of quartz from amorphous SiO₂ for pressures up to 6 GPa. We observe a sharp peak in growth rate—implying a minimum in viscosity—at 3 GPa, which we interpret as evidence that the critical pressure is being traversed. The corresponding depth below the Earth's surface at which this peak occurs (~100 km)

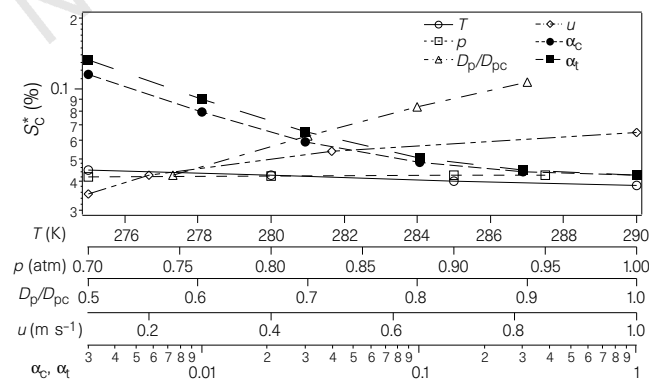


Figure 3 A study of the sensitivity of S_c^* to various parameters. The base case value is 0.042%, which is lower than most of the values plotted. Temperature and pressure cause the smallest changes, whereas updraft velocity and the accommodation coefficients are more important. The specified diameter causes the greatest change in the value of S_c^* . D_{pc} is the critical diameter; that is, the size at which the particle is considered to be activated. The base case, where D_p is that at 100% relative humidity, corresponds to $D_p/D_{pc} = 0.577$.